HHS Public Access

Author manuscript

Angew Chem Int Ed Engl. Author manuscript; available in PMC 2018 February 13.

Published in final edited form as:

Angew Chem Int Ed Engl. 2017 February 13; 56(8): 2156–2161. doi:10.1002/anie.201611774.

Micromotors spontaneously neutralize gastric acid for pH-responsive payload release

Jinxing Li, **Pavimol Angsantikul**, **Dr. Wenjuan Liu**, **Dr. Berta Esteban-Fernández de Ávila**, **Dr. Soracha Thamphiwatana**, **Prof. Mingli Xu**, **Elodie Sandraz**, **Dr. Xiaolei Wang**, **Dr. Jorge Delezuk**, **Dr. Weiwei Gao**, **Prof. Liangfang Zhang**, and **Prof. Joseph Wang**

University of California San Diego, 9500 Gilman Drive, La Jolla, CA 92093, USA

Abstract

The highly acidic gastric environment creates a physiological barrier for using therapeutic drugs in the stomach. While proton pump inhibitors have been widely used for blocking acid-producing enzymes, this approach can cause various adverse effects. Herein, we report on a new microdevice, consisting of magnesium-based micromotors that can autonomously and temporally neutralize gastric acid through efficient chemical propulsion in the gastric fluid by rapidly depleting the localized protons. Coating these micromotors with a cargo-containing pH-responsive polymer layer leads to autonomous release of the encapsulated payload upon gastric-acid neutralization by the motors. Testing in a mouse model, the in vivo results demonstrate that these motors can safely and rapidly neutralize gastric acid and simultaneously release payload without causing noticeable acute toxicity or affecting the stomach function, with the normal stomach pH restored within 24 h post motor administration.

Graphical Abstract

Magnesium-based micromotors can autonomously and temporally neutralize gastric acid through efficient chemical propulsion in the gastric fluid by rapidly depleting the localized protons. The *in vivo* results demonstrate that these motors can safely and rapidly neutralize gastric acid and simultaneously release payload without causing noticeable acute toxicity or affecting the stomach function, with the normal stomach pH restored within 24 h post motor administration.

Correspondence to: Liangfang Zhang; Joseph Wang.

Supporting information for this article, including experimental details and supporting videos, is given *via* a link at the end of the document.

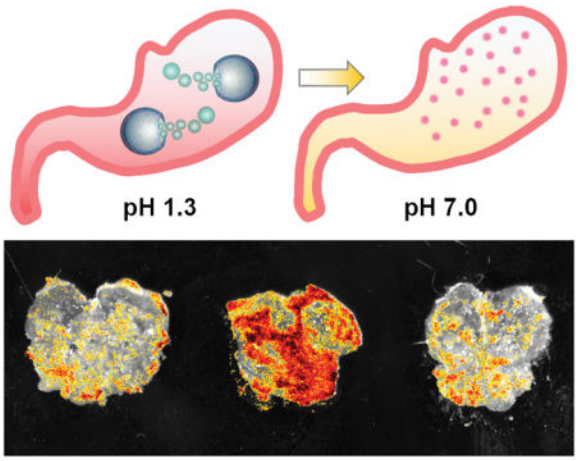

Keywords

micromotor; gastric acid; proton pump inhibitor; responsive release; drug delivery

Gastric acid, consisting primarily of hydrochloric acid produced by parietal cells in the gastric glands, plays a crucial role in maintaining the stomach's digestive function. It enables gastric proteolysis by denaturing proteins from food for break down by digestive enzymes. It also inhibits the growth of many microorganisms that enter the stomach and thus reduces the risk of pathogen infection. However, the harsh gastric environment becomes a double-edged sword at certain circumstances. For example, it creates a physiological barrier for the use and delivery of therapeutic drugs, such as protein-based drugs and some antibiotics in the stomach. In these cases, the drugs are exclusively combined with a proton pump inhibitor (PPI), which reduces the production of gastric acid. The effectiveness of PPI is attributed to the irreversible binding to the proton pumps to suppress acid secretion for approximately 12 to 24 hours.[1,2] Long-term use of PPI can cause adverse effects such as headache, diarrhea and fatigue, and in more serious scenarios cause anxiety and depression, as well as server reaction rhabdomyolysis.[3–8] Therefore, it would be highly desirable to develop alternative approaches that can temperately neutralize gastric acid while not causing adverse drug effect.

Recent advances in nanotechnology has led to the design of a variety of nanocarrier systems that can respond to various biological stimuli such as pH for triggered release of their payload.[9–12] In particular, the emerging synthetic nano/micromotors which are tiny devices that convert locally supplied fuels or externally provided energy to force and movement,[13–22] have shown considerable promise as delivery vehicles because of their active transport capacity and ability to dynamically respond to their surroundings.[23–30] For example, recent *in vivo* evaluations of synthetic micromotors demonstrated that these artificial motors can self-propel in the stomach and intestinal fluids for enhanced retention and targeted delivery in the gastrointestinal tract.[31,32] These prior studies demonstrate that the motor-based active transport systems offer attractive features for localized targeted delivery.

In this work, we introduce a new magnesium (Mg)-based micromotor, covered by a pH sensitive polymer coating, which can rapidly yet transiently neutralize the acidity of the stomach fluid *in vitro* and *in vivo*. By using acid as fuel, these synthetic motors rapidly deplete protons while propelling in the stomach, which can effectively elevate the gastric pH to neutral in less than 20 min from the motors are applied. More importantly, the motor-induced neutralization of the stomach fluid further triggers the autonomous payload release from the pH-sensitive polymer coating. In contrast to acid suppression by PPIs, the micromotors temporally alter the local environment, without blocking the function of the proton pumps. Therefore, this approach has minimal interference upon the function of the stomach and completely eliminates all possible adverse effects associated with conventional PPIs. Since the micromotors are made of biocompatible materials without biological activities, they are safe to use and will not cause acute toxicity. Compared to conventional pH-responsive nanocarriers that passively respond to the local environment, these micromotors can actively adjust their surroundings to reach desired conditions for triggered payload release. Therefore, the use of micromotors, with built-in dual capabilities of acid neutralization and pH-responsive payload release, is a unique and highly promising platform for drug delivery to treat various gastric diseases.

Figure 1a schematically illustrates the structure of a Mg-based micromotor along with its gastric acid neutralization process (through proton depletion enabled by the micromotor reaction and propulsion) and consequent payload release from the pH-responsive polymer coating. The new microvehicle thus consists of the Mg motor, the pH-sensitive polymer coating, and the encapsulated cargo. It offers multiple capabilities and functions including movement, acid neutralization, cargo transport and release. The Mg engine converts the acid fuel to propulsion force and simultaneously alters the local pH that causes payload release from the pH-sensitive coating. The core of the micromotor is made of a Mg microsphere with a diameter of ~20 μm. For the fabrication of the micromotors, a layer of Mg microparticles was dispersed onto a glass slide, followed by an asymmetrical coating of the microspheres by sputtering with a thin (10 nm) gold (Au) layer, which is responsible for efficient propulsion through the macrogalvanic corrosion of the Mg surface.[33] After sputtering the Au layer, the Janus microspheres were coated with a pH-sensitive polymeric (EUDRAGIT® L100-55, dissolves at pH > 5.5) film containing the payload. Finally, the well-separated Mg Janus micromotors were obtained after soft mechanical scratching of the glass slide, leaving a small opening that exposes the Mg surface to reaction with the gastric fluid that leads to the hydrogen-bubble generation and propulsion. The presented micromotor design is highly bio-compatible, as magnesium is an essential mineral needed for variety of physiological functions.[34] The enteric polymer coating has been extensively used for drug delivery and release,[32] while gold is commonly employed for imaging and therapeutic applications.[35] The bottom section of Figure 1a illustrates the *in vivo* acid neutralization process associated with the propulsion of the Mg-based Janus micromotors along with the corresponding payload release from the pH-sensitive polymer layer. Upon contact with the gastric fluid, a spontaneous reaction between the Mg microsphere motor surface and the surrounding protons (displayed in top left part of Figure 1a), generates hydrogen bubbles, and efficient micromotor thrust. Such reaction and acid neutralization are

facilitated by the presence of the Au layer, which boosts proton depletion through macrogalvanic corrosion.

Figure 1b shows the characterization of the Mg-based Janus micromotors. The scanning electron microscopy (SEM) image shows a small opening (~2 μm) presented on the spherical Mg-based micromotor, produced during the coating process of the micromotors, to expose the Mg surface for reaction with the surrounding acid fluid. The presence of Mg, Au, and carbon (from the polymer coating) is also confirmed by the corresponding energy-dispersive X-ray spectroscopy (EDX) mapping. The microcopy image in Figure 1c (captured from Supporting Video 1) illustrates the micromotor movement in gastric fluid simulant (pH 1.3). Efficient hydrogen bubble generation propels the micromotor with an average speed of 60 μm/s, indicating that these micromotors can rapidly react and move in gastric fluid.

The ability of Mg micromotors to neutralize gastric acid and trigger release of their payload was first tested *in vitro*. Figure 2a displays the time-dependent pH neutralization process associated with the built-in proton consumption during the reaction and propulsion of Mg micromotors in simulated gastric fluid (initial pH 1.3), using 2.75 mg of micromotors and 3 mL gastric fluid. The pH of the fluid increases rapidly from 1.3 to 6.2 within 12 min, and then more slowly, stabilizing around pH 7.5 after 18 min. These data confirm that a fast neutralization of gastric acid can be realized within less than 20 min, compared to 1 h typically required by using PPIs to reach the same level of neutralization.[1] Fluorescent pH indicator BCECF was also used to verify the fast pH neutralization of the gastric fluid by the micromotors. As displayed in Figure 2b, in the absence of Mg micromotors, the gastric fluid containing the BCECF indicator displays a light yellow color and very weak fluorescence intensity, indicative of acidic conditions. In contrast, an obvious color change to red is observed 20 min after adding the Mg micromotors to the gastric fluid; the fluorescence intensity drastically increases a similar level of that observed in a PBS buffer (pH 7.4) as a control solution. These results demonstrate that the Mg micromotors can rapidly neutralize the gastric fluid through fast proton depletion and efficient propulsion. The fast neutralization process reflects the dramatic fluid convection induced by the collective motion of micromotors in the gastric fluid and the corresponding bubble generation. Such motor-induced “self-stirring” has been shown to accelerate environmental decontamination processes.[36]

To study the pH-responsive release, enabled by the active neutralization of the gastric fluid, R6G dye was used as a model payload encapsulated within the pH-sensitive EUDRAGIT® L100-55 polymeric coating of the Mg micromotors. Inert polystyrene (PS) microspheres (diameter: 10 μm) coated with the R6G dye-loaded polymer layer was used as a control group. Figure 2c displays the payload release profile, obtained by measuring the supernatant fluorescence intensity, using the micromotors and inert (control) particles placed in the acidic gastric fluid (initial pH 1.3). The pH change associated with the presence of the Mg micromotors results in sustained release of R6G from the pH-sensitive polymeric coating. The fluorescence of the gastric fluid solution thus increases gradually and reaches a plateau at 20 min. In contrast, no such R6G release is observed using the inert PS microparticles that do not react with the protons to cause a pH change and thus the pH-sensitive polymer coating remains stable.

The fluorescence microscopy image of Figure 2d (captured from Supporting Video 2) displays the real-time propulsion and payload release of R6G from a Mg micromotor in the gastric fluid. The strong fluorescence signals observed on the micromotor body and the yellow bubble tail confirm the gradual dissolution of the polymer and consequent release of R6G. Figure 2e shows the corresponding fluorescence photographs of R6G in 1 mL bulk gastric solution in the presence of Mg micromotors and inert control microparticles (both coated with R6G-loaded pH-sensitive polymer), respectively. These images clearly show that the dye is released to the solution using micromotors but resides in the sediment at the bottom (containing the inert microparticles). This behavior indicates that the Mg micromotors, which actively neutralize the gastric fluid, can trigger drug release. This represents a distinct advantage of the autonomous micromotor-based delivery concept, over conventional stimuli-responsive drug release systems, as the micromotors themselves actively create the desired environment (stimuli) essential to trigger the release.

The *in vivo* study of Mg micromotors was further conducted by using a mouse model. In the study, the pH neutralization process was investigated by administrating different amounts of Mg micromotors (0, 2.5 mg, 5 mg and 10 mg) to four groups of mice (n=3 for each group). Upon oral administration for 20 min, the mice were euthanized and their stomach pH values were measured immediately using a microelectrode sensor coupled with a pH meter (as illustrated in Figure 3a). A 20-min time point was selected based on the *in vitro* study that has shown the Mg micromotors were able to effectively neutralize gastric acid within this time window. As shown in Figure 3b, this experiment resulted in a clear dose-dependent gastric pH change. Herein, 5 mg of Mg micromotors was able to neutralize gastric acid in the mouse stomach, resulting in pH=7.81±0.38. This motor concentration was higher than the 2.75 mg per 3 mL gastric acid as observed in the *in vitro* study. Such increase of motor amount was likely due to the continuous secretion of gastric acid from gastric glands in the mouse stomach, as well as the dynamic peristalsis wave of the stomach tissue that counteracts and dilutes the pH neutralization efficacy of the micromotors. Lower and higher doses of Mg micromotors resulted in slightly acidic and alkaline stomach environments (pH 4.24 for 2.5 mg Mg micromotors and pH 9.43 for 10 mg Mg micromotors, respectively). Using deionized (DI) water as a control resulted in a constant acidic stomach pH (1.88), which further supports that no pH neutralization occurs in the absence of Mg micromotors. Since 5 mg of Mg micromotors can neutralize the gastric acid to about neutral value in the mouse stomach, this motor dosage was chosen for further studies.

Next, we studied the *in vivo* pH-responsive payload release by orally administrating fluorescently labeled Mg micromotors. DiD was chosen as a model drug, and was loaded in the pH-sensitive polymer coating. After 20 min administration, the entire stomach was excised and cut opened along the greater curvature for fluorescence imaging. As shown in Figure 3c, the stomach from mice treated with 5 mg Mg micromotors displays strong and evenly distributed fluorescence intensity over the entire stomach, reflecting the pH change due to the proton depletion by the active Mg micromotors. Apparently, the Mg micromotor delivery system can actively tune the stomach environment to facilitate dissolution of pH-sensitive polymer and release of the payload. In contrast, mice treated with an equal amount of inert PS microparticles displays only some small local areas of the stomach with low fluorescence signal, similar to the fluorescence signal observed using the DI water control,

reflecting the self-fluorescence of the administered food. As expected, the inert PS microparticles do not alter the stomach pH, and hence cannot trigger dissolution of the pH-sensitive polymer and consequent payload release. Overall, in agreement with the early *in vitro* results, Figure 3. demonstrates the ability of Mg micromotors to neutralize gastric acid in the stomach of live animals and trigger the dissolution of the pH-responsive polymer coating with the consequent payload release. The micromotor thus serves as a motile carrier that enhances transport of its payload to different locations. The efficient local propulsion, along with the corresponding bubble tail, have shown to generate an effective convective fluid transport, to substantially enhance the delivery of cargo compared to passive-diffusion systems..[36–37] Furthermore, the propulsion of Mg micromotors provides a driving force to penetrate the mucus layer and enhance the payload retention in the stomach, which has been illustrated in early micromotor studies within the stomach and GI tract.[31,32]

To ensure the recovery of gastric pH after Mg micromotor treatment, the pH of stomach content was measured at 20 min and 24 h after administration of the motors (Figure 4a). After the pH change induced by Mg micromotor, the mean gastric pH returned to 2.16 within 24h post-treatment which is close to pH 1.88 of control group treated with DI water. To further confirm the *in vivo* recovery of gastric pH, the pH indicator BCECF with a pKa~ 6.98 was employed. The stomachs were dissected along the greater curvature and excess gastric content was removed. BCECF fluorescence dye was evenly distributed and mixed with the gastric content on the stomach tissues. Fluorescence imaging of BCECF was performed on the different treatment groups (Figure 4b). When the environmental pH is greater than its pKa, BCECF exhibits strong fluorescence emission, as shown by the stomach sample treated with micromotors for 20 min. In contrast, 24 h after administrating the Mg micromotors, the gastric content labeled with BCECF indicator showed weak fluorescence intensity, reflecting the low pH condition. The results from Figure 4a–b designate the transient pH neutralization effect of the Mg micromotors and that the normal acidity of gastric content can be recovered following the motor treatment.

Finally, the gastric toxicity of the administrated Mg micromotors was evaluated. Mice were orally administered with 5 mg of Mg micromotor or DI water and monitored for general toxicity symptoms every 2 h for the first 10 h post-administration. No observable signs of pain such as hunched posture, unkempt fur, or lethargy were observed in both groups. The Mg micromotor’s toxicity was further investigated by histological analysis. Hematoxylin and eosin (H&E) stained cross-section of glandular stomach from the micromotor-treated group showed intact glandular mucosa with no signs of superficial degeneration of columnar epithelial cells or erosion (Figure 5a). There was no observable difference in the crypt and villus size and number, or mucosal thickness, between the motor-treated and water-treated groups. Moreover, lymphocitic infiltration into the mucosa and submucosa was not apparent, implicating no sign of gastric inflammation. The potential toxicity of the Mg micromotors was further evaluated using gastric tissue sections by a terminal deoxynucleotidyl transferase-mediated deoxyuridine triphosphate nick-end labeling (TUNEL) assay to examine the level of gastric epithelial apoptosis as an indicator of gastric mucosal homeostasis. No apparent increase in gastric epithelial apoptosis was observed for micromotor-treated groups as compared to the water control group (Figure 5b). Overall, the in vivo toxicity studies demonstrate no interference in gastric pH homeostasis, and no

apparent gastric histopathologic change or inflammation, suggesting that the oral administration of Mg micromotors is safe in a mouse model. The Mg micromotors can thus temporarily adjust the stomach pH without adverse effects, making them an attractive vehicle for gastric drug delivery.

We have demonstrated that acid-powered micromotors can operate as an active microdevice to efficiently and temporarily adjust local physiological parameters *in vivo* for diverse biomedical applications. In particular, the reaction of the motor's magnesium core with the gastric fluid leads to rapid proton depletion and thus acid neutralization without affecting the normal stomach function or causing adverse effects, making these synthetic micromotors an attractive alternative to proton pump inhibitors. The fast and efficient neutralization reflects the localized fluid convection generated by the micromotor movement. When coupled to a pH-sensitive payload-containing polymer coating, this pH change can lead to autonomous release of the encapsulated cargo. The new microvehicle thus combines self-propulsion, acid neutralization, along with cargo transport and release. Its Mg engine converts the acid fuel to propulsion force and simultaneously alters the local pH that leads to payload release from the pH-sensitive coating, Such micromotor-based delivery vehicle can thus actively adjust the local environment to achieve desired conditions for triggered payload release.

Experimental Section

See supporting information.

Supplementary Material

Refer to Web version on PubMed Central for supplementary material.

Acknowledgments

L.J., P.A., W.L. and B.A. contributed equally to this work. This work is supported by the Defense Threat Reduction Agency Joint Science and Technology Office for Chemical and Biological Defense (Grant Numbers HDTRA1-13-1-0002 and HDTRA1-14-1-0064) and by the National Institute of Diabetes and Digestive and Kidney Diseases of NIH(Award Number R01DK095168). W.L. and M.X. acknowledge the China Scholarship Council (CSC) for the financial support.

References

1. Olbe L, Carlsson E, Lindberg P. Nat Rev Drug Discov. 2003; 2:132–139. [PubMed: 12563304]
2. Richardson P, Hawkey CJ, Stack WA. Drugs. 1998; 56:307–335. [PubMed: 9777309]
3. Moayyedi P, Leontiadis GI. Nat Rev Gastroenterol Hepatol. 2012; 9:132–139. [PubMed: 22330810]
4. Ho PM, Maddox TM, Wang L, Finn SD, Jesse RL, Peterson ED, Rumsfeld JS. JAMA. 2009; 301:937–944. [PubMed: 19258584]
5. Sheen E, Triadafilopoulos G. Dig Dis Sci. 2011; 56:931–950. [PubMed: 21365243]
6. Yang YX, Lewis JD, Epstein S, Metz DC. JAMA. 2006; 296:2947–2953. [PubMed: 17190895]
7. Blume H, Donath F, Warnke A, Schug BS. Drug Safety. 2006; 29:769–784. [PubMed: 16944963]
8. Juurlink DN, Gomes T, Ko DT, Szmitko PE, Austin PC, Tu JV, Henry DA, Kopp A, Mamdani MM. CMAJ. 2009; 180:713–718. [PubMed: 19176635]
9. Ganta S, Devalapally H, Shahiwala A, Amiji M. J Control Release. 2008; 126:187–204. [PubMed: 18261822]
10. Lu Y, Aimetti AA, Langer R, Gu Z. Nat Rev Mater. 2016; 1:16075.

11. Mura S, Nicolas J, Couvreur P. Nat Mater. 2013; 12:991–1003. [PubMed: 24150417]
12. Peer D, Karp J, Hong S, Farokhzad O, Margalit R, Langer R. Nat Nanotechnol. 2007; 2:751–760. [PubMed: 18654426]
13. Wang, J. Nanomachines: Fundamentals and Applications. Wiley-VCH; Weinheim: 2013.
14. Guix M, Mayorga-Martinez CC, Merkoçi A. Chem Rev. 2014; 114:6285–6322. [PubMed: 24827167]
15. Sánchez S, Soler L, Katuri J. Angew Chem Int Ed. 2015; 54:1414–1444.
16. Mei YF, Solovev AA, Sanchez S, Schmidt OG. Chem Soc Rev. 2011; 40:2109–2119. [PubMed: 21340080]
17. Palagi S, Mark AG, Reigh SY, Melde K, Qiu T, Zeng H, Parmeggiani C, Martella D, Sanchez-Castillo A, Kapernaum N, Giesselmann F, Wiersma DS, Lauga E, Fischer P. Nat Mater. 2016; 15:647–653. [PubMed: 26878315]
18. Li J, Rozen I, Wang J. ACS Nano. 2016; 10:5619–5634. [PubMed: 27219742]
19. Wilson DA, Nolte RJM, van Hest JCM. Nat Chem. 2012; 4:268–274. [PubMed: 22437710]
20. Wang H, Pumera M. Chem Rev. 2015; 115:8704–8735. [PubMed: 26234432]
21. Li J, Gao W, Dong R, Pei A, Sattayasamitsathit S, Wang J. Nat Commun. 2014; 5:5026. [PubMed: 25248549]
22. Mallouk TE, Sen A. Scientific American. 2009; 300:72–77.
23. Gao W, Kagan D, Pak OS, Clawson C, Campuzano S, Chuluun-Erdene E, Shipton E, Fullerton E, Zhang L, Lauga E, Wang J. Small. 2012; 8:460–467. [PubMed: 22174121]
24. Wu ZG, Wu YJ, He WP, Lin XK, Sun JM, He Q. Angew Chem Int Ed. 2013; 52:7000–7003.
25. Mou F, Chen C, Zhong Q, Yin Y, Ma H, Guan J. ACS Appl Mater Interfaces. 2014; 6:9897–9903. [PubMed: 24869766]
26. Abdelmohsen L, Nijemeisland M, Pawar G, Janssen GJA, Nolte RJM, van Hest JCM, Wilson D. ACS Nano. 2016; 10:2652–2660. [PubMed: 26811982]
27. Teo WZ, Pumera Martin. Chem Eur J. 2016; 22:14796. [PubMed: 27492631]
28. Moo JGS, Wang H, Pumera M. Chem Eur J. 2016; 22:355. [PubMed: 26526004]
29. Wu Z, Lin X, Wu Y, Si T, Sun J, He Q. ACS Nano. 2014; 8:6097–6105. [PubMed: 24806430]
30. Wu Z, Lin X, Si T, He Q. Small. 2016; 12:3080–3093. [PubMed: 27073065]
31. Gao W, Dong R, Thamphiwatana S, Li J, Gao W, Zhang L, Wang J. ACS Nano. 2015; 9:117–123. [PubMed: 25549040]
32. Li J, Thamphiwatana S, Liu W, Esteban-Fernandez de Avila B, Angsantikul P, Sandraz E, Wang J, Xu T, Soto F, Ramez V, Wang X, Gao W, Zhang L, Wang J. ACS Nano. 2016; 10:9536–9542.
33. Gao W, Feng X, Pei A, Gu Y, Li J, Wang J. Nanoscale. 2013; 5:4696–4700. [PubMed: 23640547]
34. Vormann J. Mol Aspects Med. 2003; 24:27–37. [PubMed: 12537987]
35. Daniel MC, Astruc D. Chem Rev. 2004; 104:293–346. [PubMed: 14719978]
36. Orozco J, Cheng G, Vilela D, Sattayasamitsathit S, Vazquez-Duhalt R, Valdés-Ramírez G, Pak OS, Escarpa A, Kan C, Wang J. Angew Chem Int Ed. 2013; 125:13518–13521.
37. Wu Z, Li J, de Ávila BEF, Li T, Gao W, He Q, Zhang L, Wang J. Adv Funct Mater. 2015; 25:7497–7501.

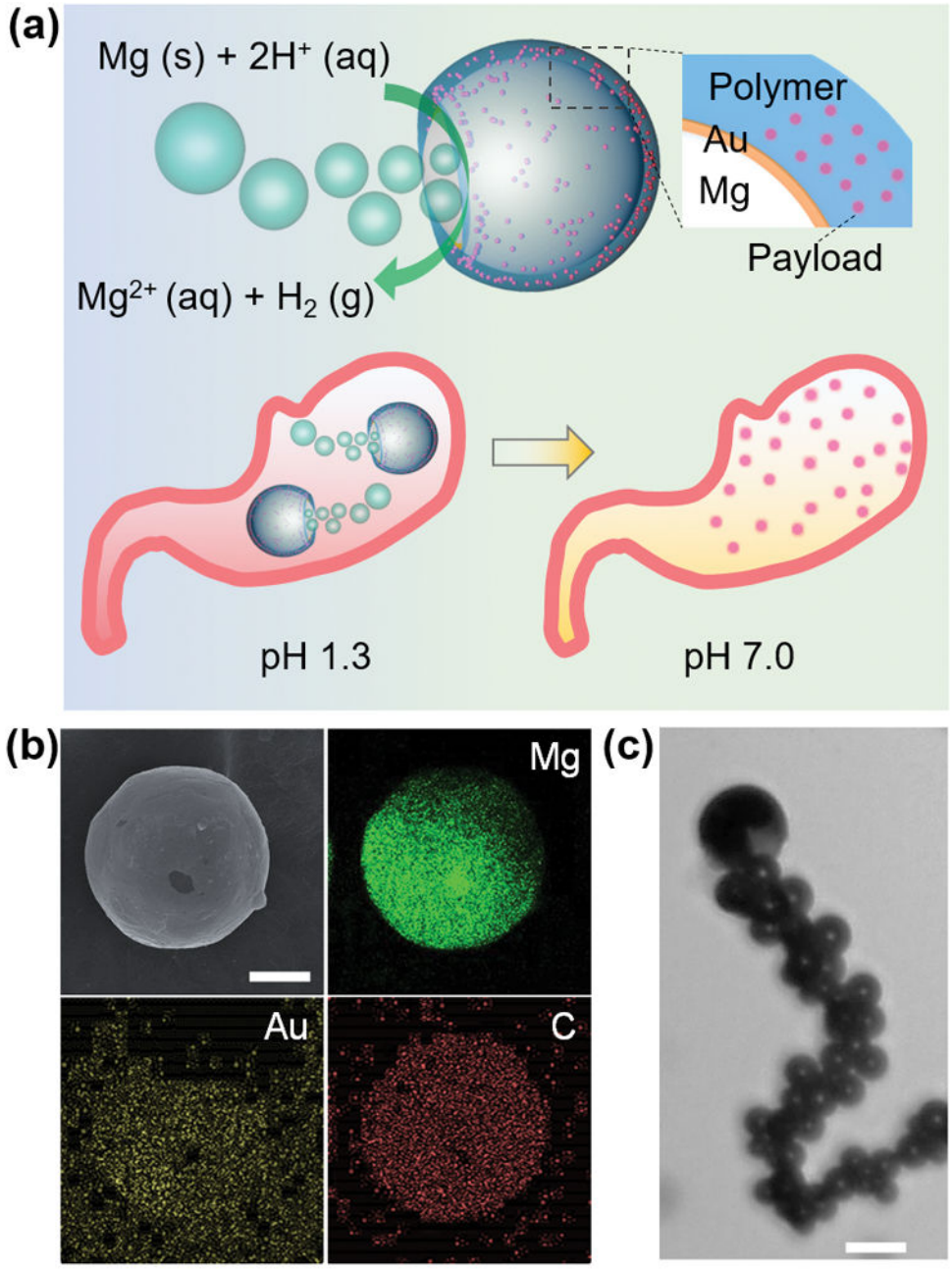

Figure 1.

(a) Schematic illustrations of an acid-powered magnesium (Mg)-based micromotor and its acid neutralization mechanism. The micromotor is made of a Mg microsphere coated with a thin gold (Au) layer and a payload-encapsulated pH-sensitive polymer layer. A tiny opening exposes the Mg surface to outside environment. At acidic pH, the Mg reacts with acids, which generates hydrogen bubbles, propels the motors, and depletes protons in the solution. This process spontaneously causes pH increase and release of payloads from the pH-responsive polymer layer. (b) SEM and EDX characterizations of the Mg-based micromotor.

Scale bar: 5 μm. (c) Microscopy image illustrating the bubble propulsion of a micromotor in gastric fluid (Supplementary Movie 1). Scale bar: 20 μm.

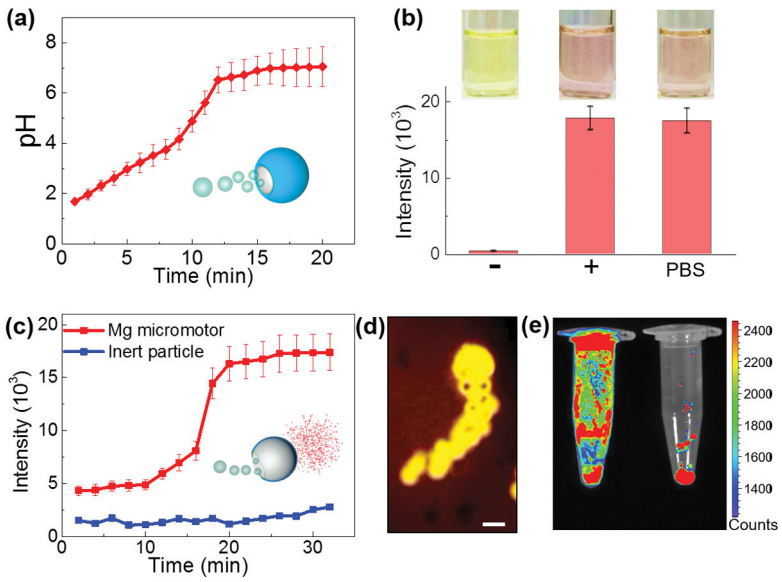

Figure 2.

In vitro acid neutralization and pH-triggered payload release. (a) Time-dependent pH value of gastric fluid (3 mL, pH 1.3) in the presence of Mg micromotors (2.75 mg). (b) Fluorescence intensity of a pH indicator BCECF in gastric fluid (pH 1.3), gastric fluid containing 2.75 mg of Mg micromotors, and PBS buffer (pH 7.4), respectively. Insets: images of the corresponding solutions. (c) Time-dependent fluorescence intensity of released rhodamine 6G (R6G) in the supernatant of 3 mL gastric fluid. R6G dye is loaded in the pH-sensitive polymer coating (starts to dissolve at pH > 5.5) as a model payload. Polystyrene (PS)-based inert microparticles with a similar size as the Mg micromotors were used as a negative control. (d) Fluorescence image showing the propulsion and release processes of an R6G-loaded Mg micromotor. Scale bar: 20 μm. (e) Fluorescence images of the released R6G in the supernatant of gastric fluid containing Mg micromotors (left) or PS microparticles (right).

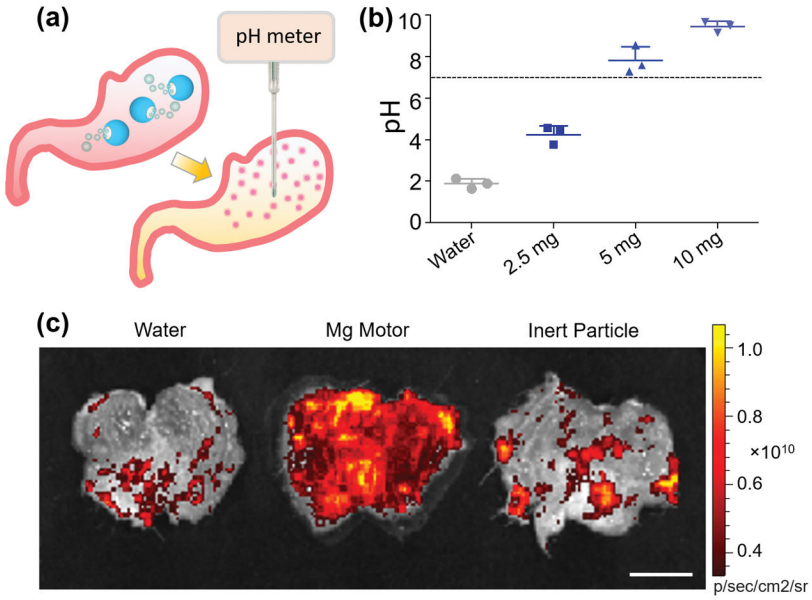

Figure 3.

In vivo acid neutralization and pH-triggered payload release. (a) Schematic illustration of *in vivo* gastric acid neutralization process by Mg micromotors and pH measurement using a microelectrode-enabled pH meter. (b) *In vivo* gastric pH values using a mouse model (n=3) measured 20 min post administration of different amounts of Mg micromotors. DI water was used as a negative control. (c) Superimposed fluorescent images of the whole stomach of mice collected 20 min post administration of DI water, Mg micromotors, or inert PS microparticles (both Mg micromotors and PS microparticles are loaded with DiD dye which is encapsulated in the pH-sensitive polymer coating as a model drug). Scale bars: 5 mm.

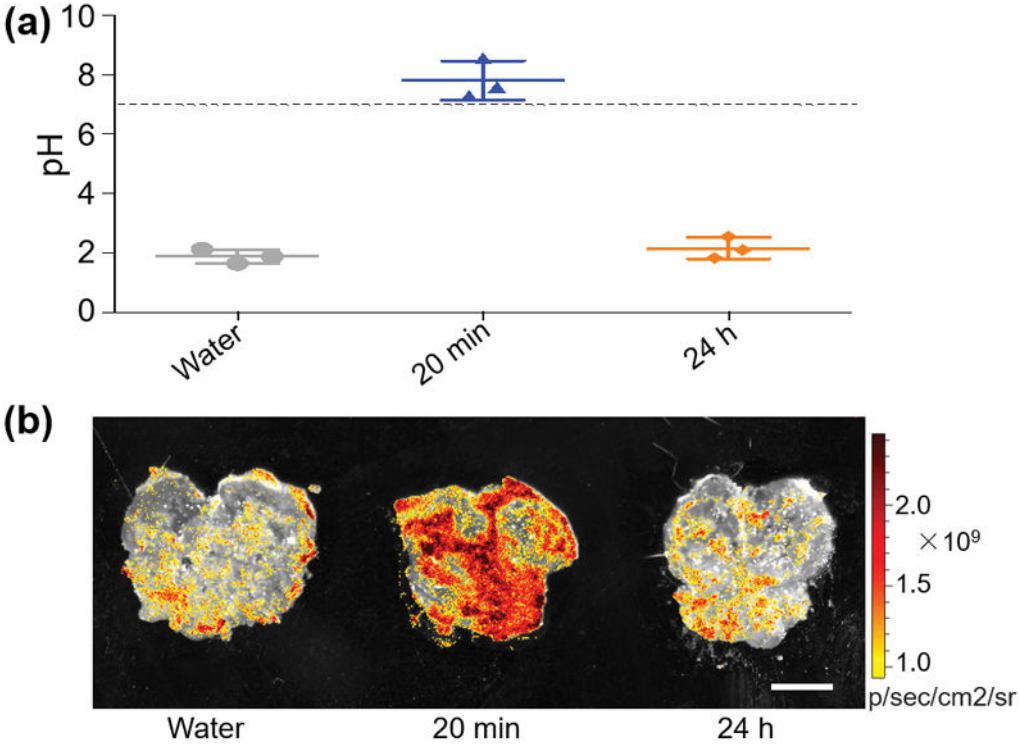

Figure 4.

Recovery of the gastric pH post micromotor treatment. (a) In vivo gastric pH values using a mouse model (n=3) measured 20 min and 24 h post administration of 5 mg of Mg micromotors. Mice administrated with water were used as a control. (b) Fluorescent images of the pH indicator BCECF superimposed on the entire stomach for the samples in (a).

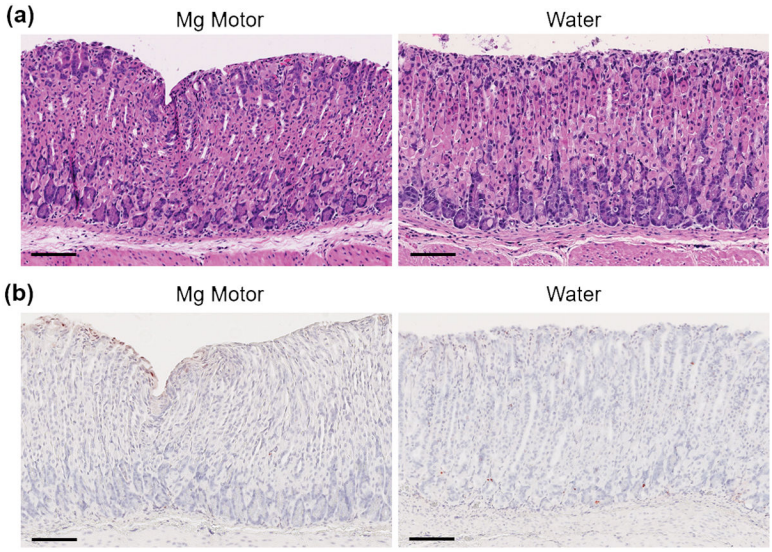

Figure 5.

Toxicity evaluation of Mg micromotors. Mice were orally administered with 5mg of Mg micromotors or DI water. After 24 h, mice were sacrificed and sections of the mouse stomach were processed and stained with (a) H&E assay or (b) TUNEL assay. Scale bars, 100 μm.